

CO/FTIR Spectroscopic Characterization of Pd/ZnO/Al₂O₃ Catalysts for Methanol Steam Reforming

V. Lebarbier · R. Dagle · T. Conant · J. M. Vohs ·
A. K. Datye · Y. Wang

Received: 10 December 2007 / Accepted: 18 January 2008 / Published online: 12 February 2008
© Springer Science+Business Media, LLC 2008

Abstract An as-synthesized 8.8wt% Pd/ZnO/Al₂O₃ catalyst was either pretreated under O₂ at 773 K followed by H₂ at 293 K or under H₂ at 773 K to obtain, respectively, a supported metallic Pd⁰ catalyst (Pd⁰/ZnO/Al₂O₃) or a supported PdZn alloy catalyst (PdZn/ZnO/Al₂O₃). Both catalysts were studied by CO adsorption using FTIR spectroscopy. For the supported PdZn alloy catalyst (PdZn/ZnO/Al₂O₃), exposure to a mixture of methanol and steam, simulating methanol steam reforming reaction conditions, does not change the catalyst surface composition. This implies that the active sites are PdZn alloy like structures. The exposure of the catalyst to an oxidizing environment (O₂ at 623 K) results in the break up of PdZn alloy, forming a readily reducible PdO with its metallic form being known as much less active and selective for methanol steam reforming. However, for the metallic Pd⁰/ZnO/Al₂O₃ catalyst, FTIR results indicate that metallic Pd⁰ can transform to PdZn alloy under methanol steam reforming conditions. These results suggest that PdZn alloy, even after an accidental exposure to oxygen, can self repair to form the active PdZn alloy phase under methanol steam reforming conditions. Catalytic behavior of the PdZn/ZnO/

Al₂O₃ catalyst also correlates well with the surface composition characterizations by FTIR/CO spectroscopy.

Keywords FTIR spectroscopy · Pd catalyst · PdZn alloy catalyst · Methanol steam reforming

1 Introduction

Based on the current rate of consumption of fossil fuels, most of these resources could be depleted in a few decades [1]. A movement toward the generation of renewable energy is imperative. Proton-Exchange Membrane Fuel Cells (PEMFCs) powered by hydrogen from renewable sources to produce electricity appear to be an alternative solution. Hydrogen fuel can be obtained from steam reforming of alcohols such as methanol. Methanol is an attractive candidate due to its high hydrogen/carbon ratio, low sulfur content [2, 3], low cost [3, 4], relatively low reforming temperature (473–623 K) [2–5], easy storage feasibility [6] and high availability [4, 7].

Methanol steam reforming is catalyzed by supported metals [8–15]. Many studies [16–28] have focused on copper-based catalysts which exhibit a high reactivity and favorable selectivity to CO₂ and H₂. However, the Cu-based catalysts can readily undergo deactivation at high temperature [29] (≥553 K) due to metal sintering and their pyrophoric nature makes them undesirable for safe and efficient operation of PEM fuel cells. PdZn catalysts, on the other hand, do not have the disadvantages of Cu-based catalysts and have attracted much attention recently [9, 10, 12, 14, 30–38]. Iwasa et al. [11, 39] showed that Pd/ZnO catalysts reduced at high temperatures (>573 K) are very active and selective to H₂ and CO₂. The high catalytic performance of Pd/ZnO catalysts was attributed to the

V. Lebarbier · R. Dagle · Y. Wang (✉)
Pacific Northwest National Laboratory, Richland,
WA 99354, USA
e-mail: yongwang@pnl.gov

V. Lebarbier · T. Conant · A. K. Datye
Department of Chemical and Nuclear Engineering,
University of New Mexico, Albuquerque, NM 87106, USA

J. M. Vohs
Department of Chemical and Biomolecular Engineering,
University of Pennsylvania, Philadelphia, PA 19104, USA

presence of PdZn alloy, as revealed by the combination of XRD, XPS and TPR methods [9, 39]. According to Iwasa et al. [39] the PdZn alloy is formed during the reduction under H_2 at a temperature higher than 573 K. Metallic Pd^0 , on the other hand, predominantly produces CO and H_2 via methanol decomposition. Since their pioneering work, several papers [12, 31, 36, 40–43] have investigated the alloying effect on the reactivity of the Pd/ZnO catalysts. Chin et al. [44] studied the reactivity of a 16.7% Pd/ZnO catalyst which only has metallic Pd^0 . The results showed a continuous increase in methanol conversion during the first half hour to a steady state conversion of 32%. The corresponding CO selectivity decreased from 47% to 14% throughout the experiment. It was proposed that the bimetallic PdZn alloy, responsible for the activity changes, was formed under reaction conditions. In agreement with these findings, recent results from Conant et al. [45], illustrated a modification of the PdZn nanoparticle surface affected by the reducing/oxidizing environment and the reactions conditions. However, the surface compositions of either metallic Pd^0 or PdZn alloy under methanol steam reforming or oxidizing conditions have not been studied yet. The purpose of the present study is twofold: (1) to understand the influence of the methanol steam reforming and oxidizing conditions on the surface composition of PdZn alloy; and (2) to investigate the potential PdZn alloy formation from the metallic Pd^0 under methanol steam reforming conditions.

2 Experimental

2.1 Preparation of the Catalyst

An 8.8wt% Pd/ZnO/ Al_2O_3 (Pd relative to Pd/ZnO/ Al_2O_3) catalyst was prepared by multiple incipient wetness impregnations. Specifically, a palladium nitrate solution (4.4 wt% Pd, Aldrich) was mixed with a $Zn(NO_3)_2 \cdot 6H_2O$ (99.5%, Aldrich). The premixed Pd and Zn nitrate solution (Pd:Zn molar ratio 0.38) was added drop by drop to the alumina support (boehmite from Sasol) calcined at 1,123 K for 5 h prior to the multiple impregnations. A total of five impregnations were used. Between each impregnation step, the powder was dried at 353 K for 2 h. A Pd:Zn ratio of 0.38 was chosen since it is optimum ratio for methanol steam reforming based on our previous report [33].

2.2 Infrared Spectroscopy

IR spectra were recorded with a Nicolet Magna 750 spectrometer, equipped with a MCT detector (resolution: 4 cm^{-1} , 128 scans). The sample pressed into a pellet (ca.

30 mg for a 1.32 cm^2 pellet) was activated using two different pretreatment methods. The first pretreatment method reduces the catalyst under H_2 for 2 h at 773 K. The second pretreatment includes the calcination of catalyst under O_2 for 2 h at 773 K, followed by first cooling the sample under vacuum to 293 K and then reduced under H_2 at 293 K for 2 h. During the oxidation (or reduction) treatment, the sample was alternatively exposed to O_2 (or H_2) for 4 min and evacuated under vacuum for 2 min to simulate flow conditions. After these pretreatments, CO adsorption was conducted at 293 K. For some of the experiments, CO was then evacuated under vacuum at 623 K and a mixture of $H_2O + CH_3OH$ (molar ratio 1.8:1), was introduced into the cell for 30 min at 548 K (5 cycles: $H_2O + CH_3OH$ for 4 min and evacuation under vacuum for 2 min). This step was followed by an evacuation under vacuum at 623 K and a CO adsorption at 293 K. For each CO adsorption, 1.1 μmol of gas was introduced.

2.3 Reactivity

Methanol steam reforming activity was evaluated in a 4 mm I.D quartz tube reactor. Approximately 200 mg of catalyst was loaded between two layers of quartz wool inside the reactor. A thermocouple was placed in the middle of the catalyst bed. A pre-mixture feed of water/methanol (molar ratio of 1.8:1), was aerated through a vaporizer operating at 643 K and introduced into the reactor using a syringe pump. Nitrogen purge was fed into the system using a Brooks Mass Flow Controller (5850E series). The nitrogen consisted of 29% of the total vapor feed (molar). Total throughput was run at GHSV = $21,845\text{ h}^{-1}$ at a temperature of 548 K. Prior to activity tests, the catalyst was reduced in-situ under 10% H_2/N_2 at 623 K for 2 h. A glass condenser at 273 K was used to separate liquid products from gaseous products. The product gases, CO, CO_2 and H_2 were separated using MS-5A and PPQ columns and analyzed on-line by means of a MTI Quad Micro GC (Model Q30L) equipped with a TCD.

3 Results and Discussion

3.1 CO Adsorption

Based on our previous work [33, 40] and that of others [39], reduction temperatures higher than 573 K are sufficient to reduce the supported and unsupported Pd/ZnO to form PdZn alloy. Therefore, a PdZn alloy catalyst, designated as PdZn/ZnO/ Al_2O_3 , was obtained by reducing the 8.8% Pd/ZnO/ Al_2O_3 catalyst under H_2 at 773 K for 2 h. To identify the surface compositions of PdZn alloy that are

prevalent under the methanol steam reforming conditions, infrared spectra of CO adsorbed on the PdZn alloy catalyst before and after the exposure to a mixture of methanol and steam at 548 K were measured and are shown in Fig. 1 (spectra a and b). To study the potential surface composition change of PdZn alloy and its correlation with the stability of PdZn alloy in the presence of O₂ under a typical methanol steam reforming temperature, infrared spectrum of CO adsorbed on PdZn alloy catalyst after the exposure to O₂ at 623 K was also measured and is included in Fig. 1 (spectrum c).

In Fig. 1, both spectra a and b are similar. They both show a main band at 2,071 cm⁻¹ characteristic of linear CO adsorption. A small band between 2,000–1,800 cm⁻¹, due to multibonded CO species, is also noted. According to our previous HREELS results on the Zn/Pd(111) alloy surfaces and the FTIR results on a similar high surface area PdZn/ZnO/Al₂O₃ catalyst [38], the band situated at 2,071 cm⁻¹ is ascribed to the vibration of CO linearly adsorbed on the PdZn alloy particles. It is also worth noting that the area of the band at 2,071 cm⁻¹ for both spectra a and b is almost identical. Therefore, these results indicate that the surface composition of the PdZn alloy catalyst is not affected by the exposure to a mixture of methanol and steam at a typical methanol steam reforming temperature of 548 K. In other words, the surface composition of the PdZn alloy is likely the active composition for methanol steam reforming.

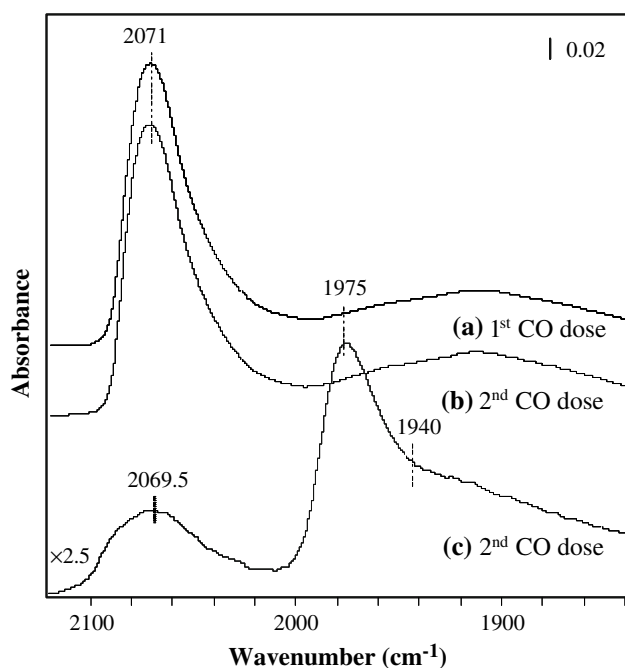


Fig. 1 FTIR spectra recorded after CO adsorption, (a) just after pretreatment under H₂, (b) after exposure to H₂O/CH₃OH and (c) after oxidation, for the PdZn/ZnO/Al₂O₃ catalyst. Spectra are normalized to a pellet of 100 mg

The spectrum c in Fig. 1 was recorded after the PdZn alloy catalyst was exposed to O₂ at 623 K. It has a main band at 1,975 cm⁻¹ and a shoulder at 1,940 cm⁻¹ in addition to a band at ~2,069.5 cm⁻¹, which are unlike the spectra a and b where the band at 2,071 cm⁻¹ due to linear CO adsorption on PdZn alloy dominates. IR bands at similar positions were previously observed on a 2.77% Pd/Al₂O₃ catalyst (i.e. 2,069, 1,981 and 1,936 cm⁻¹) [46] and were assigned to the $\nu(\text{CO})$ mode of CO adsorbed on Pd⁰. Our separate HREELS results on Pd(111) and FTIR results on a high surface area Pd catalysts also suggest that the bands at 1,975 cm⁻¹ and 2,069.5 cm⁻¹ are indicative of CO adsorbed in bridging and atop sites on the Pd, respectively. Therefore, we can deduce that the IR sample collected for spectrum c has the properties of metallic Pd⁰. Exposure of the PdZn alloy to oxygen at 623 K likely broke up the PdZn alloy to form PdO, which is known to be readily reduced to form the metallic Pd⁰ either due to the evacuation of the IR sample at 623 K and/or because of the exposure of the IR sample to CO for the IR measurement. In other words, exposure of the PdZn alloy to oxygen under a methanol steam reforming temperature can lead to the break up of the active PdZn alloy phase to PdO, which can be readily reduced to form the metallic Pd⁰. As discussed above, metallic Pd⁰ is known to dominate the decomposition of methanol.

To study the surface composition change of metallic Pd⁰ under the methanol steam reforming reaction conditions, infrared spectra of CO adsorption on a supported metallic Pd⁰ catalyst before and after the exposure to a mixture of methanol and steam at 548 K were measured and are shown in Fig. 2 (spectra a and b). The supported metallic Pd⁰ catalyst, designated as Pd⁰/ZnO/Al₂O₃, was obtained by calcining the 8.8% Pd/ZnO/Al₂O₃ catalyst under O₂ at 773 K for 2 h followed by a reduction under H₂ at 293 K for 2 h. Based on our previous work [41] and that of others [13, 47], such a pretreatment Pd⁰ results in the formation of a mostly metallic Pd⁰/ZnO/Al₂O₃ catalyst. The spectrum a in Fig. 2 has two bands at 2,062 and 1,980 cm⁻¹ and a shoulder at 1,940 cm⁻¹. As discussed above on the spectrum c in Fig. 1, these bands are attributed to the vibration of CO coordinated to metallic Pd⁰ supported on ZnO/Al₂O₃. Spectrum b in Fig. 2 recorded after introduction of the H₂O + CH₃OH mixture is quite different than spectrum a. It has a main band at 2,073 cm⁻¹, characteristic of atop or linear CO adsorption, and a small band between 2,000 and 1,800 cm⁻¹, due to multibonded CO species. The band at 2,073 cm⁻¹ is characteristic of bimetallic PdZn alloy, as discussed above, for spectra a and b in Fig. 1. Metallic Pd⁰ catalyst can be formed by either a mild reduction as in the case of the Pd⁰/ZnO/Al₂O₃ catalyst or decomposition of PdZn alloy in the presence of O₂ followed by a mild reduction as in the case of the catalyst

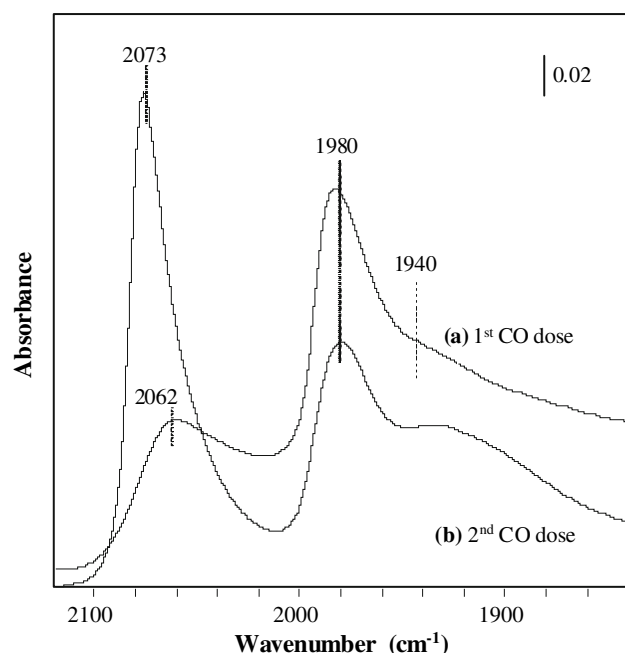


Fig. 2 FTIR spectra recorded after CO adsorption, (a) under O_2 at 773 K + H_2 at 293 K and (b) under H_2 at 773 K after exposure to H_2O/CH_3OH , for the metallic $Pd^0/ZnO/Al_2O_3$ catalyst. Spectra are normalized to a pellet of 100 mg

measured in Fig. 1 spectrum c. The results in Fig. 2 indicate that under the methanol steam reforming conditions, metallic Pd can transform to the PdZn alloy which is the active phase for methanol steam reforming. Hydrogen produced during methanol steam reforming may facilitate the PdZn alloy formation. In our previous report, a continuous increase in methanol conversion accompanied with a continuous decrease in CO selectivity were observed on a supported metallic Pd^0/ZnO catalyst [44], likely due to the PdZn alloy formation from Pd and ZnO under the methanol steam reforming conditions according to the FTIR results discussed here.

3.2 Reactivity

The above FTIR results suggest that in the presence of O_2 the active PdZn alloy phase can break up to form PdO, which is readily to be reduced to form the much less active and selective metallic Pd^0 while the metallic Pd can self-repair and transform to the active PdZn alloy phase under methanol steam reforming conditions. To correlate these FTIR observations with the activity measurement, a supported PdZn alloy catalyst, $PdZn/ZnO/Al_2O_3$, was studied for methanol steam reforming. This catalyst was first studied in methanol steam reforming at 548 K for 2 h, then purposely exposed to an air flow at 623 K for 1/2 h, and followed by re-evaluating its methanol steam reforming

activity at 548 K. Figure 3 shows the methanol conversion and CO selectivity as a function of time on stream. For the first 2 h time-on-stream (i.e. before oxidation), the CH_3OH conversion and the CO selectivity are $\sim 77\%$ and 2.3%, respectively, as expected from the catalytic performances on a PdZn alloy catalyst. The CO selectivity is below the equilibrium value (5.6%). These results are in agreement with the FTIR data displayed in Fig. 1 a and b showing that the surface composition of PdZn alloy is not modified by the methanol steam reforming conditions.

After catalyst was exposed to air, a marked decrease in methanol conversion (60%) and an increase in CO selectivity (76%) were initially observed, which is in sharp contrast to those measured before the catalyst was exposed to air, i.e., 77% and 2.3%, respectively. The initial poor methanol conversion and CO selectivity are due to the presence of metallic Pd, which is formed from the PdZn alloy break up in the presence of oxygen followed by a mild reduction according to the FTIR results discussed above (spectrum c in Fig. 1), and metallic Pd^0 is well known to possess a poor methanol steam reforming activity [11, 15]. From Fig. 3 we can also see that methanol conversion increases and CO selectivity decreases with the time-on-stream. The gradual increase of the CH_3OH conversion and the corresponding decrease of the CO selectivity are attributed to the continuous formation of PdZn alloy from the metallic Pd^0 under methanol steam reforming as supported by the FTIR results in Fig. 2. Therefore, metallic Pd^0 formed due to the decomposition of PdZn alloy in the presence of oxygen can self-repair and re-form the active PdZn alloy phase under the methanol steam reforming conditions.

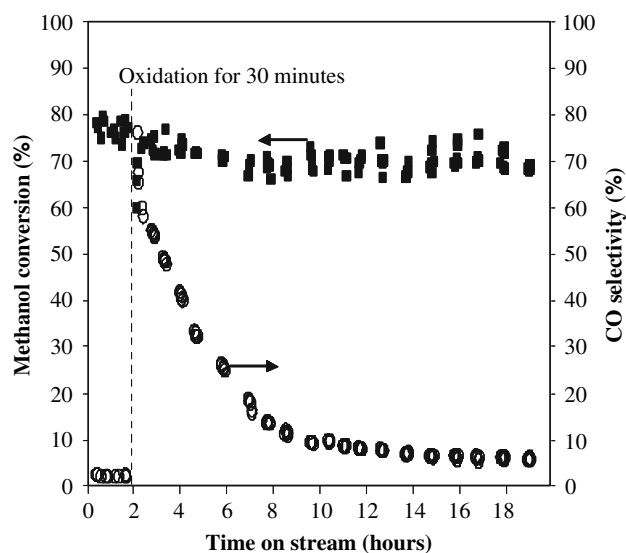


Fig. 3 Methanol conversion and CO selectivity versus time on stream (minutes) for a 8.8% $Pd/ZnO/Al_2O_3$ catalyst ($T = 548$ K, GHSV = 21,845 h^{-1})

4 Conclusion

In this study, we examined the effects of gaseous environment on the surface composition of a 8.8% Pd/ZnO/Al₂O₃ catalyst using CO-FTIR spectroscopy. The gaseous environment was chosen to simulate that during methanol steam reforming and after an accidental exposure to oxygen. It was found that the surface composition of the active PdZn alloy is not affected by the exposure to methanol steam reforming conditions, and the active phase in methanol steam reforming is likely the PdZn alloy. Exposure of the active PdZn alloy to oxygen can lead to the break up of PdZn alloy to readily reducible PdO with its metallic form being known as much less active and selective for methanol steam reforming. However, the metallic Pd⁰ can form the active PdZn alloy phase again under the methanol steam reforming conditions.

Acknowledgments This work was performed in the Environmental Molecular Sciences Laboratory, a national scientific user facility sponsored by the U.S. Department of Energy's Office of Biological and Environmental Research, located at Pacific Northwest National Laboratory in Richland, WA. We greatly acknowledge funding for this work provided by the U.S. Department of Energy (Grant no. DE-FG02-05ER15712).

References

1. DIREM/Industrie pétrolière en (2005) <http://www.industrie.gouv.fr/energie/petrole/textes/explo-pro-monde05.html>
2. Brown LF (2001) *Int J Hydrogen Energy* 243:420–427
3. Rostrup-Nielsen JR (2001) *Phys Chem Chem Phys* 3:283–288
4. Lindström B, Pettersson LJ (2001) *Int J Hydrogen Energy* 26:923–933
5. Peters R, Düsterwald HG, Höhle B (2000) *J Power Sources* 86:507–514
6. Yong ST, Hidajat K, Kawi S (2004) *J Power Sources* 131: 91–95
7. Lindström B, Pettersson LJ (2002) *J Power Sources* 106:264–273
8. Takahashi K, Kobayashi H, Takezawa N (1985) *Chem Lett* 759–762
9. Iwasa N, Mayanagi T, Nomura W, Arai M, Takezawa N (2003) *Appl Catal A Gen* 248:153–160
10. Iwasa N, Yoshikawa M, Nomura W, Arai M (2005) *Appl Catal A Gen* 292:215–222
11. Iwasa N, Kudo S, Takahashi H, Masuda S, Takezawa N (1993) *Catal Lett* 19:211–216
12. Ranganathan ES, Bej SK, Thompson LT (2005) *Appl Catal A Gen* 289:153–162
13. Takezawa N, Iwasa N (1997) *Catal Today* 36:45–56
14. Suwa Y, Ito S-I, Kameoka S, Tomishige K, Kunimori K (2004) *Appl Catal A Gen* 267:9–16
15. Iwasa N, Takezawa N (2003) *Top Catal* 22:215
16. Agrell J, Biggersson H, Boutonnet M (2002) *J Power Sources* 106:249–257
17. Pour V, Barton J, Benda A (1975) *Collect Czech Chem Commun* 40:2923
18. Barton J, Pour V (1980) *Collect Czech Chem Commun* 45:3402
19. Kobayashi H, Takezawa N, Minochi C (1981) *J Catal* 69:487
20. Takahashi H, Takezawa N, Kobayashi H (1982) *Appl Catal* 2:363
21. Santacesaria E, Carrà S (1983) *Appl Catal* 5:345
22. Jiang CJ, Trimm MS, Wainwright NW (1993) *Appl Catal A Gen* 97:145
23. Breen JP, Ross JRH (1999) *Catal Today* 51:521
24. Peppley BA, Amphlett JC, Kearns LM, Mann RF (1999) *Appl Catal A Gen* 179:21–29
25. Agarwal V, Patel S, Pant KK (2005) *Appl Catal A Gen* 279: 155–164
26. Yu X, Tu S-T, Wang Z, Qi Y (2005) *J Power Sources* 150:57–66
27. Frank B, Jentoft FC, Soerijanto H, Kröhnert J, Schlögl R, Schomäcker R (2007) *J Catal* 246:177–192
28. Mastalir A, Patzkó A, Frank B, Schomäcker R, Ressler T, Schlögl R (2007) *Catal Commun* 8:1684–1690
29. Twigg M, Spencer M (2003) *Top Catal* 22:192
30. Hong C-T, Yeh C-T, Yu F-H (1989) *Appl Catal* 48:385–396
31. Kim C-H, Lee JS, Trimm DL (2003) *Top Catal* 22:319
32. Cao C, Xia G, Holladay J, Jones E, Wang Y (2004) *Appl Catal A Gen* 262:19–29
33. Xia G, Holladay JD, Dagle RA, Jones EO, Wang Y (2005) *Chem Eng Technol* 28:515
34. Valdés-Solís T, Marbán G, Fuertes AB (2006) *Catal Today* 116:354–360
35. Lenarda M, Moretti E, Storaro L, Patrono P, Pinzari F, Rodríguez-Casellón E, Jiménez-López A, Busca G, Finocchio E, Montanari T, Frattini R (2006) *Appl Catal A Gen* 312:220–228
36. Dagle RA, Chin Y-H, Wang Y (2007) *Top Catal*. doi: 10.1007/s11244-007-9009-4
37. Palo DR, Dagle RA, Holladay JD (2007) *Chem Rev* accepted
38. Jeroro E, Lebarbier V, Datye A, Wang Y, Vohs J-M (2007) *Surf Sci* 601:5546–5554
39. Iwasa N, Masuda S, Ogawa N, Takezawa N (1995) *Appl Catal A Gen* 125:145–157
40. Hu J, Wang Y, Vanderwiel D, Chin C, Palo D, Rozmiarek R, Dagle R, Cao J, LHolladay J, Baker E (2003) *Chem Eng J* 93: 55–60
41. Chin Y-H, Dagle R, Hu J, Dohnalkova AC, Wang Y (2002) *Catal Today* 77:79–88
42. Karim A, Conant T, Datye A (2006) *J Catal* 243:420–427
43. Karim A (2006) PhD Thesis. University of New Mexico, New Mexico
44. Chin Y-H, Wang Y, Dagle R, Li XS (2003) *Fuel Process Technol* 83:193–201
45. Conant T, Karim A, Lebarbier V, Wang Y, Girgsdies F, Schlögl R, Datye A (2007) *J Catal* submitted
46. Skotak M, Karpinski Z, Juszczak W, Pielaszek J, Kepinski L, Kazachkin DV, Kovalchuk VI, d'Itri JL (2004) *J Catal* 227:11–25
47. Iwasa N, Ogawa N, Masuda S, Takezawa N (1998) *Bull Chem Soc Jpn* 71:1451–1455